

INTRASEASONAL VARIABILITY OF THE SOUTH  
ASIAN MONSOON

by

DAVID MICHAEL LAWRENCE

B.S., University of California at San Diego, 1993

M.S., University of Colorado, 1996

A thesis submitted to the  
Faculty of the Graduate School of the  
University of Colorado in partial fulfillment  
of the requirements for the degree of  
Doctor of Philosophy  
Program in Atmospheric and Oceanic Sciences

1999

This thesis entitled:  
Intraseasonal Variability of the South Asian  
Monsoon  
written by David Michael Lawrence  
has been approved for the Program in Atmospheric  
and Oceanic Sciences by

---

Peter J. Webster

---

Andrew M. Moore

Date \_\_\_\_\_

The final copy of this thesis has been examined by the signatories, and we find that both the content and the form meet acceptable presentation standards of scholarly work in the above mentioned discipline.

Lawrence, David Michael (Ph. D., Astrophysical, Planetary, and  
Atmospheric Sciences)

Intraseasonal Variability of the South Asian Monsoon

Thesis directed by Professor Peter J. Webster

The South Asian monsoon exhibits pronounced intraseasonal variability on timescales ranging from a few days to more than a month. A principal purpose of this study is to provide a comprehensive analysis of low-frequency monsoon intraseasonal variability and to determine its structure in space and time. Large-scale active and break periods of rainfall are associated with the slowly evolving Intraseasonal Oscillation (ISO) that is characterized during northern summer by an apparent northward movement of convection emanating from the central equatorial Indian Ocean. The evolution of ISO convection can be thought of in terms of propagating equatorial modes. Surface frictional convergence into a Rossby cell that is excited by equatorial ISO convection generates a band of convection that is oriented southeast to northwest and stretches from the equator to about 20°N. Viewed along any meridian the mode appears to propagate northward while equatorial convection propagates to the east.

Interannual variations of summertime ISO activity are investigated and are found to be related to year-to-year changes in the number of discrete events. Seasons of high ISO activity exhibit significantly more low precipitation days and consequently deficient seasonal rainfall than seasons characterized by little or no ISO activity. ISO activity is found to be uncorrelated to the El Niño-Southern Oscillation (ENSO) or any other contemporaneous sea surface temperature (SST) variability. The summertime ISO activity does exhibit a reasonably strong inverse

relationship with South Asian monsoon strength. The year-to-year variations of ISO activity also exhibit a dominant biennial timescale.

A second dominant mode of intraseasonal variability is made up of synoptic-scale westward propagating convective disturbances with timescales between 5 and 10 days. During the active ISO phase over India, westward propagating synoptic-scale wave activity is above normal. The development of high-frequency convective disturbances over the Bay of Bengal and peninsular India is attributed to instability that is favored in regions of strong easterly vertical wind shear in conjunction with equatorial heating. As ISO convection moves into the western Pacific Ocean region westward propagating synoptic-scale waves are excited from which point they propagate to the west across southeast Asia into the Bay of Bengal bringing episodes of significant rainfall during the suppressed, and normally dry, ISO phase over India.

## ACKNOWLEDGMENTS

First and foremost, I would like to thank my advisor, Professor Peter Webster, who provided the motivation and direction for this work. The freedom to pursue a number of my own ideas, often down the wrong path, was invaluable in my professional development. Additionally, Peter provided me the opportunity to take part in the Joint Air-Sea Monsoon INteraction Experiment (JASMINE) on board the NOAA Ship the Ronald H. Brown in the Bay of Bengal, which was an enlightening highlight of my graduate school career.

Thanks also to my thesis committee members: Peter Webster, George Kiladis, Andy Moore, Jerry Meehl, Bob Grossman, and Jeff Forbes for their time and expertise.

Special thanks to George Kiladis and Harry Hendon whose work and knowledge inspired a good portion of the work of this thesis. Gil Compo, Matt Wheeler, and Chris Torrence helped out immensely with discussions on statistical techniques. Thanks also to Bob Tomas, Kamran Sahami, Johannes Loschnigg, Brian Mapes, Paquita Zuidema, John Fasullo, Jeff Hicke, Cristina Perez, and Christy Oelfke Clark for many rewarding discussions. I would also like to thank Murry Salby for his excellent teaching of dynamics and spectral analysis, Peter Webster and Judy Curry for their excellent and thought provoking introductions to the field, and Andy Moore for his role in bringing the Forecasting Weather and Climate class to the CDC Friday afternoon weather and climate discussion sessions (and, on a completely tangential note, Jim Corbridge for his thought-provoking course on water law).

I would like to thank the PAOS office staff, especially Bonnie Grebe, Kelly Duong, Robert Lambeth, Sherry Yearsley, and Lois Macaria.

I would also like to thank Hai-Ru Chang and Kamran Sahami who continually solved problems, particularly mine, with the computer system while the parade of sys-ops came and went. The computing was done at the PAOS Computing Facility primarily using IDL and Fortran. The data was obtained from the NOAA Climate Diagnostic Center and the National Center for Atmospheric Research archives.

Special thanks go to the office mates both past and present for keeping things fun, including Paquita, Johannes, Kamran, Chris, Gil, Cristina, and Christy. Paquita, in particular, has been a constant source of support and enthusiasm. Johannes, has been, well, Johannes. The snack crew got me through many a slow afternoon. The mates at Edgewood: Diane, Matt, Brett, Courtney, Tim, Erin, Dave, and Adam made my time away from school just that. Life wouldn't have been the same without some great snow seasons and the 10th Mountain Division Hut system and my soccer teams, the Gunners, the Blues, the Jazz, and Scatter.

Finally, I want to thank my family who mean more to me I can express. My parents, George and Kathy, who have been so steadfastly supportive that I hardly even noticed it and thankfully convinced me to apply to CU; my brother Steve for being my best buddy; and Gram for the Scrabble games and being the best grandmother ever. Last, but no where near least, I would like to thank my long-time friend and girlfriend Diane who has an unmatched spirit and who is a pretty good copy editor to boot.

## THE MONSOON SOVEREIGN

The atmosphere was stifling: the air was still as death,  
As the parched wheels emitted their foul and charnel breath.  
A mantle of red shadow envelops all around—  
The trees, the grass, the hamlets, as the storm-clouds forward  
bound.  
Of a sudden, comes a whirlwind, dancing, spinning rapidly;  
Then gust on gust bursts quick, incessant, mad, rushing furiously.  
A crash—and the Monsoon's on us, in torrents everywhere,  
With the bellowing roar of thunder, and lightning, flare on flare.  
The tempest's now abated; a hush falls o'er the scene;  
Then myriad birds start chattering and the grass again is green,  
The fields like vast, still mirrors, in sheets of water lie,  
The frogs, in droning chorus, sing hoarse their lullaby,  
Each tank and pool is flooded, great rivers burst their banks,  
King Summer's reign is ended, the Monsoon sovereign ranks.

— L. H. Niblett (1938), adapted

## CONTENTS

### CHAPTER

1	INTRODUCTION . . . . .	1
1.1	Annual Cycle and the Mean Monsoon . . . . .	9
1.2	Variability of the South Asian Monsoon . . . . .	16
1.2.1	The Intraseasonal Oscillation . . . . .	16
1.2.2	Other Intraseasonal Variability . . . . .	18
1.2.3	Interannual Variability . . . . .	18
1.3	Summary . . . . .	21
2	DATA AND METHODS . . . . .	22
2.1	Datasets . . . . .	22
2.1.1	OLR . . . . .	22
2.1.2	NCEP/NCAR Reanalysis . . . . .	23
2.1.3	SST . . . . .	24
2.1.4	Precipitation . . . . .	24
2.2	Methods . . . . .	25
2.2.1	Statistical Techniques . . . . .	25
2.2.2	Lagged Cross-Correlation and Linear Regression . . . . .	26
3	STRUCTURE AND EVOLUTION OF THE INTRASEASONAL OSCILLATION . . . . .	30
3.1	Theories for Summertime ISO Evolution . . . . .	30
3.2	Timeseries Analysis and Temporal and Spatial Filtering . . . . .	33
3.2.1	Fourier Spectral Analysis . . . . .	33



3.2.2	Wavenumber-Frequency Analysis . . . . .	36
3.2.3	Filtering . . . . .	43
3.3	Seasonal Structure of the Planetary Scale Intraseasonal Oscillation . . . . .	45
3.3.1	Convection . . . . .	50
3.3.2	Circulation . . . . .	54
3.4	Detailed Structure of the Summer Intraseasonal Oscillation . . . . .	61
3.4.1	Separation of Modes . . . . .	68
3.4.2	Sea Surface Temperature . . . . .	74
3.5	Summary and Discussion . . . . .	78
4	INTERANNUAL VARIATIONS OF THE INTRASEASONAL OSCILLATION . . . . .	83
4.1	Interannual and Intraseasonal Variability . . . . .	83
4.2	Measures of Boreal Summer ISO Activity . . . . .	88
4.3	Monsoon Indices and Monsoon-ENSO Relationships . . . . .	98
4.3.1	Monsoon Indices . . . . .	98
4.3.2	Monsoon-ENSO Relationships . . . . .	102
4.4	Interannual Variations of ISO Activity . . . . .	104
4.4.1	Changes in ISO Characteristics . . . . .	104
4.4.2	Relation to Interannual SST Variability . . . . .	112
4.4.3	ENSO . . . . .	112
4.4.4	Other SST Variability . . . . .	116
4.4.5	Relation to Interannual South Asian Monsoon Variability . . . . .	116
4.4.6	ISO, ENSO, and the Indian Monsoon . . . . .	125

4.5	Summary and Discussion . . . . .	125
5	MODULATION OF SYNOPTIC-SCALE CONVECTION . . . . .	131
5.1	Synoptic-Scale Variability . . . . .	131
5.2	Wavenumber-Frequency Spectra . . . . .	136
5.2.1	Method . . . . .	136
5.2.2	OLR Wavenumber-Frequency Variance Spectra . . . . .	137
5.2.3	Wavenumber-Frequency Filtering . . . . .	141
5.3	Intraseasonal Oscillation and Synoptic-Scale Disturbances . . . . .	141
5.3.1	Intraseasonal Oscillation . . . . .	141
5.3.2	Synoptic-Scale Westward Propagating Waves . . . . .	144
5.3.3	Synoptic-Scale Waves and the ISO Phase . . . . .	146
5.4	Synoptic-Scale Wave Activity and ISO . . . . .	149
5.4.1	Measure of Synoptic-Scale Wave Activity . . . . .	149
5.4.2	Active ISO Phase . . . . .	154
5.4.3	Suppressed ISO Phase . . . . .	160
5.5	A Canonical Sequence . . . . .	166
6	CONCLUSIONS . . . . .	171
6.1	Summary . . . . .	171
6.2	Structure and Evolution of the ISO . . . . .	172
6.3	Interannual Variations of the Intraseasonal Oscillation . . . . .	173
6.4	Modulation of Synoptic-Scale Waves . . . . .	175
6.5	Implications for Prediction . . . . .	177
6.6	Future Work . . . . .	179
6.6.1	JASMINE . . . . .	180
	BIBLIOGRAPHY . . . . .	183

## FIGURES

### FIGURE

1.1	Precipitation Timeseries for JJAS 1987 and 1988 . . . . .	5
1.2	Spectral Analysis of OLR . . . . .	6
1.3	Climatology of OLR and 850-mb Wind . . . . .	10
1.4	Climatology of Precipitation Estimates . . . . .	11
1.5	Climatology of Zonal 200-mb Wind . . . . .	14
1.6	Climatology of SST . . . . .	15
1.7	Time-Space Sections of OLR Anomalies, Summer 1996 . . . . .	19
2.1	Cross-Correlation and Linear Regression Example . . . . .	28
3.1	Regional Spectral Analysis of OLR . . . . .	35
3.2	Wavenumber-Frequency Spectra of OLR . . . . .	37
3.3	Climatology of $OLR_{25-80}^2$ . . . . .	39
3.4	Wavenumber-Frequency Spectra of Zonal Wind and Divergence . . . . .	41
3.5	Annual Cycle Time-Latitude Diagrams of SST and $OLR_{25-80}^2$ . . . . .	42
3.6	Climatology of $OLR_{25-80}^2$ . . . . .	44
3.7	OLR, 200-mb Wind and Streamfunction Lagged Regressions . . . . .	47
3.8	OLR, 850-mb Wind and Divergence Lagged Regressions . . . . .	48
3.9	OLR, 1000-mb Wind and Divergence Lagged Regressions . . . . .	49
3.10	Regressed OLR Versus Latitude . . . . .	52
3.11	Lag-Latitude Section of Regressed OLR and 1000-mb Divergence . . . . .	53
3.12	Simple Solutions for Heat-Induced Tropical Circulation, Gill (1980) . . . . .	55

3.13	Lag-Longitude Section of Regressed OLR and $v_{1000}$ . . . . .	59
3.14	OLR and 200-mb Wind Anomalies Regressed Onto $OLR_{25-80e}$ . . . . .	62
3.15	OLR and 850-mb Wind Anomalies Regressed Onto $OLR_{25-80e}$ . . . . .	63
3.16	Lag-Space Sections of Regressed $OLR_{25-80}$ . . . . .	65
3.17	Lag-Space Sections of $OLR_{25-80}$ Segregated by Event Type . . . . .	71
3.18	Histogram of ISO Events (SN, EN, E) Per Fortnight . . . . .	73
3.19	Mean SST Basic State Difference Map of SN – EN Events . . . . .	75
3.20	Lagged SST Anomalies During SN Events . . . . .	77
3.21	Lag-Space Diagrams of SST and $OLR_{25-80}$ for SN Events . . . . .	79
4.1	Precipitation Timeseries for JJAS 1987 and 1988 . . . . .	86
4.2	Precipitation Time-Latitude Sections for JJAS 1987 and 1988 . . . . .	87
4.3	Leading Two EOF Loading Vectors for $OLR_{25-80}$ . . . . .	91
4.4	Leading Three Rotated EOF Loading Vectors for $OLR_{25-80}$ . . . . .	93
4.5	Wavelet Analysis of $OLR_{EOF}$ . . . . .	95
4.6	Wavelet Analysis of $OLR_{25-80e}$ . . . . .	96
4.7	$OLR_{25-80}$ , $OLR_{EOF}$ , and $OLR_{25-80e}$ Variance Maps . . . . .	99
4.8	AIRI-OLR Regression Map . . . . .	101
4.9	Seasonal ISO Activity Indices . . . . .	105
4.10	ISO- $OLR_{25-80}^2$ Regression Map . . . . .	107
4.11	Composite Precipitation Sextile Histogram: India . . . . .	109
4.12	Composite Precipitation Sextile Histogram: Bay of Bengal . . . . .	111
4.13	Composite Wavelet Analysis for Warm Niño3 SST Years . . . . .	113
4.14	Composite Wavelet Analysis for Cool Niño3 SST Years . . . . .	114
4.15	Regression of Global SST Anomalies Onto ISO Activity Indices . . . . .	117
4.16	Scatter Diagram of $OLR_{EOF}^2$ vs. OLR-India . . . . .	118

4.17	$[\text{OLR}_{EOF^2}]$ , AIRI, and OLR-India Comparison . . . . .	121
4.18	Composite Wavelet Analysis for Wet Asian Monsoon Years . . . . .	123
4.19	Composite Wavelet Analysis for Dry Asian Monsoon Years . . . . .	124
4.20	Regression of Mean OLR Onto $[\text{OLR}_{EOF^2}]$ and JJAS Niño3 SST . . . . .	126
4.21	Fourier Spectra of ISO Activity Indices, AIRI, and Niño3 SST . . . . .	129
5.1	Precipitation Timeseries and Time-Space Sections: Summer 1992 . . . . .	133
5.2	Wavenumber-Frequency Spectra of OLR at $10^\circ$ – $20^\circ$ N . . . . .	138
5.3	OLR and 850-mb Wind Lagged Regression Maps of ISO . . . . .	143
5.4	OLR, 850-mb Wind, and 850-mb Relative Vorticity Lagged Regression Maps of Synoptic-Scale Events . . . . .	145
5.5	$\text{OLR}_{5-10w}$ Lagged Regression Sections for Convective and Suppressed Phases of ISO . . . . .	148
5.6	$\text{OLR}_{5-10w}$ , $\text{OLR}_{5-10w}^2$ , and $\text{OLR}_{25-80e}$ for June to July 1992 . . . . .	150
5.7	Climatology of $\text{OLR}_{5-10w}$ and Zonal Vertical Wind Shear . . . . .	153
5.8	Modulation of $\text{OLR}_{5-10w}^2$ During Convective Phase of ISO . . . . .	155
5.9	Lagged Composite Timeseries of ISO, $\text{OLR}_{5-10w}^2$ , and $\text{OLR}_{5-10e}^2$ at $75^\circ$ E, $15^\circ$ N . . . . .	156
5.10	Power Spectra During Convective and Suppressed ISO Phase . . . . .	159
5.11	$\text{OLR}_{5-10w}^2$ During Suppressed ISO Phase Over India . . . . .	162
5.12	Modulation of $\text{OLR}_{5-10w}^2$ During Convective Phase of ISO over Western Pacific Ocean . . . . .	163
5.13	Lagged Composite Timeseries of ISO, $\text{OLR}_{5-10w}^2$ , and $\text{OLR}_{5-10e}^2$ at $125^\circ$ E, $15^\circ$ N . . . . .	165
5.14	Circulation Anomalies During Westward $\text{OLR}_{5-10w}^2$ . . . . .	167
5.15	Canonical Evolution of ISO and Synoptic-Scale Waves . . . . .	168

6.1 Time-Latitude Section of Meteosat-5 OLR Data During JASMINE 182

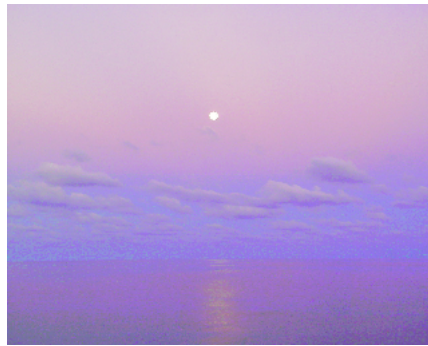
## TABLES

## TABLE

3.1	Large-Scale ISO Event Mode Characteristics . . . . .	70
4.1	Correlations Between Indian Monsoon Indices . . . . .	103
4.2	Correlations Between Seasonal ISO Activity and Indian Monsoon Indices . . . . .	120

## CHAPTER 1

### INTRODUCTION



*”Keep a register of all changes of wind and weather at all houres, by night and by day, shewing the point the wind blows from, whether strong or weak: The Rains, Hail, Snow and the like ... especially Hurricanes ... but above all to take exact care to observe the Trade-Wines, about what degrees of Latitude and Longitude they first begin, where and when they cease, or change, or grow stronger or weaker.”*

— Instructions from the Royal Society of London’s – Directions for Sea-Men, Bound for Far Voyages (1666) – indicating an early appreciation of the importance of understanding the variability of the monsoon.

The Asian summer monsoon is the most vigorous weather system in the world, profoundly affecting most of the nations of South and Southeast Asia. Across the region, over 75% of the total annual rainfall occurs during the summer monsoon. Nearly 60% of the planet’s population relies on the soaking monsoon rains to support agricultural production, to provide adequate drinking water for humans and



livestock, and to generate hydroelectric power that drives agricultural and industrial production. The significance of the monsoon in people's daily lives cannot be overestimated as emphasized by Khushwant Singh (Fein and Stephens 1987):

The monsoon is the most memorable experience in the lives of Indians ... What the four seasons of the monsoon mean to the European, the one season of the monsoon means to the Indian. The summer monsoon is preceded by desolation; it brings with it the hopes of spring; it has the fullness of summer and the fulfillment of autumn all in one. (p.38, Singh 1987)

The monsoon's influence, however, is not restricted to the Asian continent. The intense heating associated with the condensation of water vapor in the upper atmosphere impacts the circulation patterns throughout the tropics and the extra-tropics (e.g., Yasunari and Yuji 1992). Additionally, observational evidence points to a complex interrelationship between the Asian monsoon and the El Niño-Southern Oscillation (ENSO), a relationship that was first observed by Sir Gilbert Walker (1924) and that has been the subject of intense study over the last decade (for review see Webster *et al.* 1998). The relationship between Indian rainfall and the phase of ENSO is not entirely clear although there is some indication that the monsoon's role is active rather than passive (Normand 1953; Yasunari 1990). The global impacts of ENSO from both a climatological (e.g., among countless others Ropelewski and Halpert 1987; Kiladis and Diaz 1989) and a sociological perspective (e.g., Glantz 1996) are well-documented, although by no means comprehensive. If the monsoon indeed influences ENSO, then the impacts of the monsoon on global climate would be widespread. Regardless, the Asian monsoon is an important component of the tropical coupled atmosphere/ocean system and needs to be accurately represented in models in order to increase predictability on the global scale.

The Asian monsoon exhibits high amplitude variability on virtually all timescales from synoptic to interdecadal. The observed fluctuations of the monsoon have been studied for over 200 years (for historical account of South Asian monsoon studies, see Kutzbach 1987) with more intensive studies in the last 100 years motivated by a desire to understand and predict large-scale droughts such as the great Indian drought and the resulting famine of 1877. On the interannual timescale, the standard deviation of total Indian summer rainfall is only 10% of the long term mean of 853 mm (Mooley and Parthasarathy 1984). However, even such small variations in seasonal precipitation can significantly impact crop production (Parthasarathy *et al.* 1988; Gadgil 1996). For example, Webster *et al.* (1998) show that total Indian rainfall is positively correlated with Indian rice production at 0.61 over the last four decades with a 10% reduction in total rainfall leading to an average 15% reduction in rice production.

While the stress is often on how the total seasonal rainfall impacts crop production and society in general, it is events that occur within the season that often have the greatest overall impact. For example, the following is an excerpt from a Food and Agriculture Organization report on the 1996 Indian monsoon season:

Torrential monsoon rains in July over central and north eastern parts of the country caused serious flooding. Latest estimates indicate that overall 2.4 million people were affected, with some 900 people and 15,000 livestock killed. Around 3.3 million hectares of crop area were affected and 600,000 hectares severely damaged. Overall, the 1996 monsoon began on time ... providing favorable planting conditions for 1996/97 paddy and coarse grains. However, in east and west Madhya Pradesh, low rainfall in June and early July resulted in delayed planting of the main crop which may affect overall production.

Apparently, both excessive rainfall and deficient or delayed rainfall can adversely affect crop production, which highlights the need for better understanding and prediction of both the short and long term fluctuations in precipitation.

The strong intraseasonal variations in precipitation in the South Asian monsoon are obvious from inspection of daily precipitation timeseries such as those shown for the 1987 and 1988 seasons in Fig. 1.1. During 1987, there are three clear "active" periods of rainfall, which are defined in this study simply as prolonged periods of heavy precipitation over central India. The active periods are separated by "break" periods which are defined in this study as prolonged periods of low rainfall. The three 1987 active periods are separated by approximately 40 days each. The active periods of precipitation have been linked to northward moving envelopes of convection from the equatorial Indian Ocean which in turn have been linked to large-scale eastward propagating convection envelopes along the equator (e.g., Yasunari 1979; Julian and Madden 1981) (see Section 1.2.1 and Chapter 3 for further details and discussion). The entire system is termed the Intraseasonal Oscillation (ISO).

While the near 40-day variability is a dominant mode of intraseasonal variability of rainfall in the South Asian monsoon region, other timescales are important as well. For example, evidence of shorter timescale oscillations is apparent in Fig. 1.1 as heavy precipitation events separated by about 6–9 days. Both the near 40-day and the 6–9-day timescales of variability show up as statistically significant spectral peaks in outgoing longwave radiation records (Fig. 1.2).

Evidence of interannual variability is also apparent in Fig. 1.1. For this region in central India, the total precipitation was 896 mm in 1988, which is in excess of 50% more rain than the 554 mm that fell in 1987. The two years exhibit notably different intraseasonal fluctuations. While 1987 contains at least three well-defined active periods separated by well-defined break periods, 1988 appears to be essentially devoid of any obvious active or break periods except perhaps an active

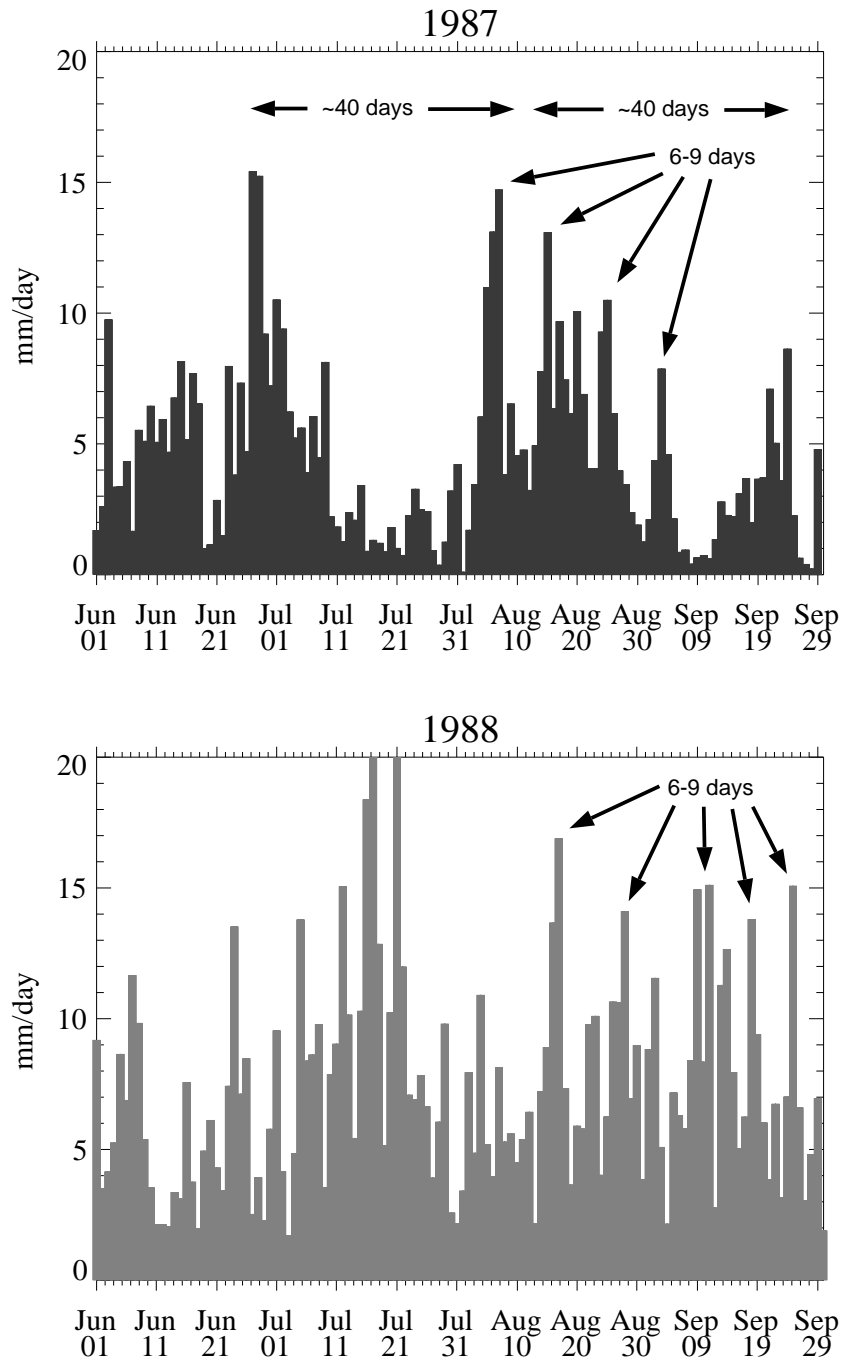


Figure 1.1. Timeseries of daily precipitation rate estimates averaged over central India (75°–80°E, 10°–15°N) for June through September, 1987 and 1988. Precipitation estimates from station data (Section 2.1.4).

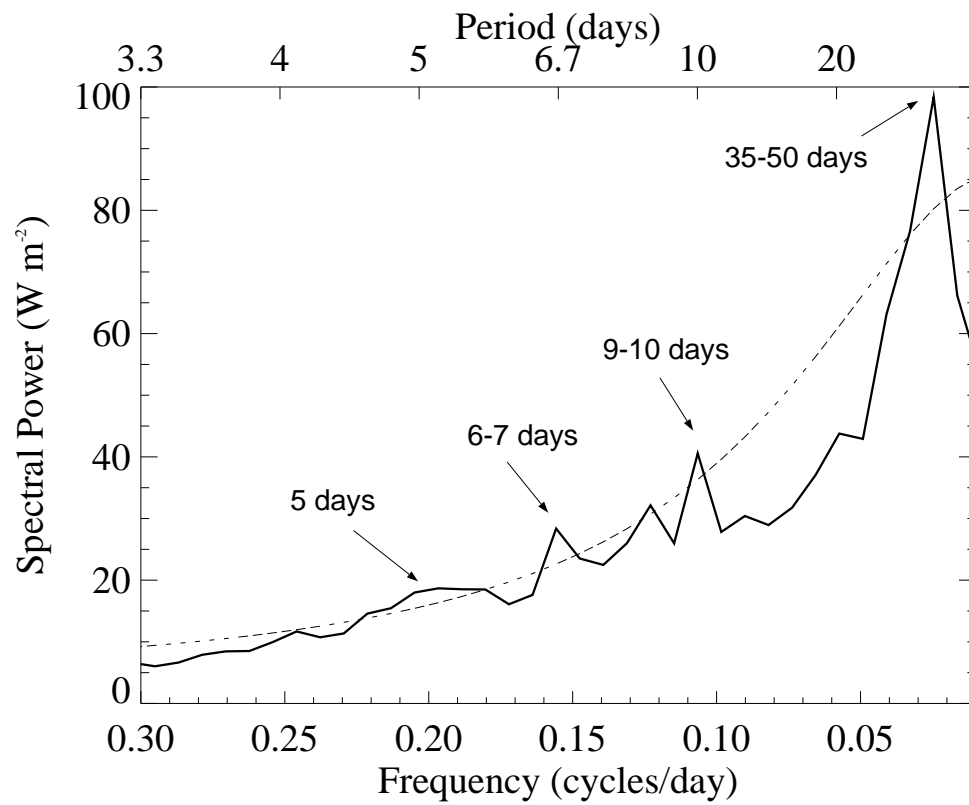


Figure 1.2. Ensemble averaged variance spectrum of June-September outgoing longwave radiation for the years 1974-1997 in the Indian peninsula region 70°–80°E, 10°–20°N. Dashed line is the 95% significance level theoretical red-noise spectrum. Data from NOAA Outgoing Longwave Radiation dataset (Section 2.1.1)

period in the middle of June. The stark differences between these two seasons in both total precipitation and the intraseasonal variability have stimulated substantial research (Krishnamurti *et al.* 1989; Krishnamurti *et al.* 1990) and are often used as measuring sticks to assess the simulation skill of GCMs.

Swaminathan (1987) suggests that the effects of abnormal monsoons on crop production and economic output could be mitigated with skillful forecasts of seasonal monsoon precipitation. Unfortunately, accurate seasonal prediction of monsoon rainfall using dynamic forecast models has proven elusive (Webster *et al.* 1998), although empirical forecasts have fared somewhat better (Shukla 1987; Das 1987). The potential reasons for poor forecast skill in the Asian monsoon region are varied. For example, Fennessy *et al.* (1994) find that GCM simulations of the Asian monsoon are highly sensitive to the formulation of orography and soil moisture. The Atmospheric Model Intercomparison Project (AMIP) compared the various atmospheric General Circulation Models (GCMs) and found that the simulated rainfall distributions over the Bay of Bengal and the Indian subcontinent varied widely between models (Lau *et al.* 1996). The lack of skill in the Asian monsoon region may be partly due to the fact that the models do not simulate well the observed northward propagation of monsoon convective zones. Even single models that capture the strong dry monsoon (1987) to wet monsoon (1988) transition show little or no predictability in other years (Sperber and Palmer 1996). Webster *et al.* (1998) argue that the high degree of spread seen in monsoon forecasts is likely due either to difficulty in modeling monsoon regions or to nonlinear error growth due to regional hydrodynamic instabilities. To answer this question, continued progress towards a more complete understanding of the complex observed variability of the

monsoon is required such that the important processes that govern monsoonal precipitation can be correctly incorporated into forecast models.

The purpose of this dissertation is to examine in detail the intraseasonal variability of the South Asian monsoon. A number of aspects of the intraseasonal variability will be addressed. The principal aims are to:

- describe the spatial and temporal structure of the summertime ISO,
- illustrate the primary similarities and differences between the summertime and wintertime ISOs,
- interpret the northward movement of summertime ISO convection in terms of equatorial waves,
- examine the relationship between year-to-year fluctuations of summertime ISO activity and interannual variations of South Asian monsoon strength, and
- investigate the modulation of synoptic-scale convection by the ISO.

The remainder of this chapter is devoted to a description of the annual cycle and the mean summertime monsoon and a review of the current understanding of the summertime ISO. Chapter 2 describes the datasets used and introduces the statistical methods used in this study. Chapter 3 presents the temporal and structural evolution of the summertime ISO and compares it to the wintertime ISO. The interannual fluctuations of summertime ISO activity are examined in Chapter 4, which also includes a more extensive review of interannual South Asian monsoon variability. The synoptic-scale variability in the South Asian monsoon region and its modulation by the ISO is investigated in Chapter 5. The final chapter provides a synthesis of the observations and conclusions as well as a brief discussion of future work.

### 1.1 Annual Cycle and the Mean Monsoon

The term "monsoon" appears to have originated from the Arabic word *mausim* which means season. The Asian monsoon system contains two distinct seasons: the "wet" and the "dry." The wet occurs during boreal summer when warm and moist winds blow across South Asia from the southwest. During the dry winter season, the winds reverse, blowing cool and dry air from the winter continent across the Indian subcontinent from the northeast (for discussion of annual cycle and fundamental physical principles required to explain monsoon circulations, see Webster 1987). The focus of this study will be on the wet summer season, but it is important to keep in mind that the summer Asian monsoon is part of the greater Asian-Australian monsoon system (Webster *et al.* 1998).

The climatological summer, June to September (JJAS), and winter, December to March (DJFM), mean distributions of 850-mb winds, outgoing longwave radiation (OLR), and precipitation are shown in Figs. 1.3 and 1.4. During northern summer, the low level circulation over the Indian Ocean and the Indian subcontinent is dominated by strong cross-equatorial flow and southwesterly winds across the Arabian Sea, the Indian subcontinent, and the Bay of Bengal. Halley (1686) first hypothesized that the cross-equatorial flow is caused by the temperature contrast between the cool southern oceans and the hot continental landmass, a land-sea temperature difference that generates a pressure gradient that drives the winds. Hadley (1735) advanced the theory of the monsoon by including the effects of the rotation of the earth which explains the characteristic southwesterly, rather than pure southerly flow. The monsoonal circulation acts as a moisture "conveyor belt," transporting moisture from the south Indian Ocean and the Arabian Sea toward the South Asian landmass and the Bay of Bengal (e.g., Cadet and Greco 1987;



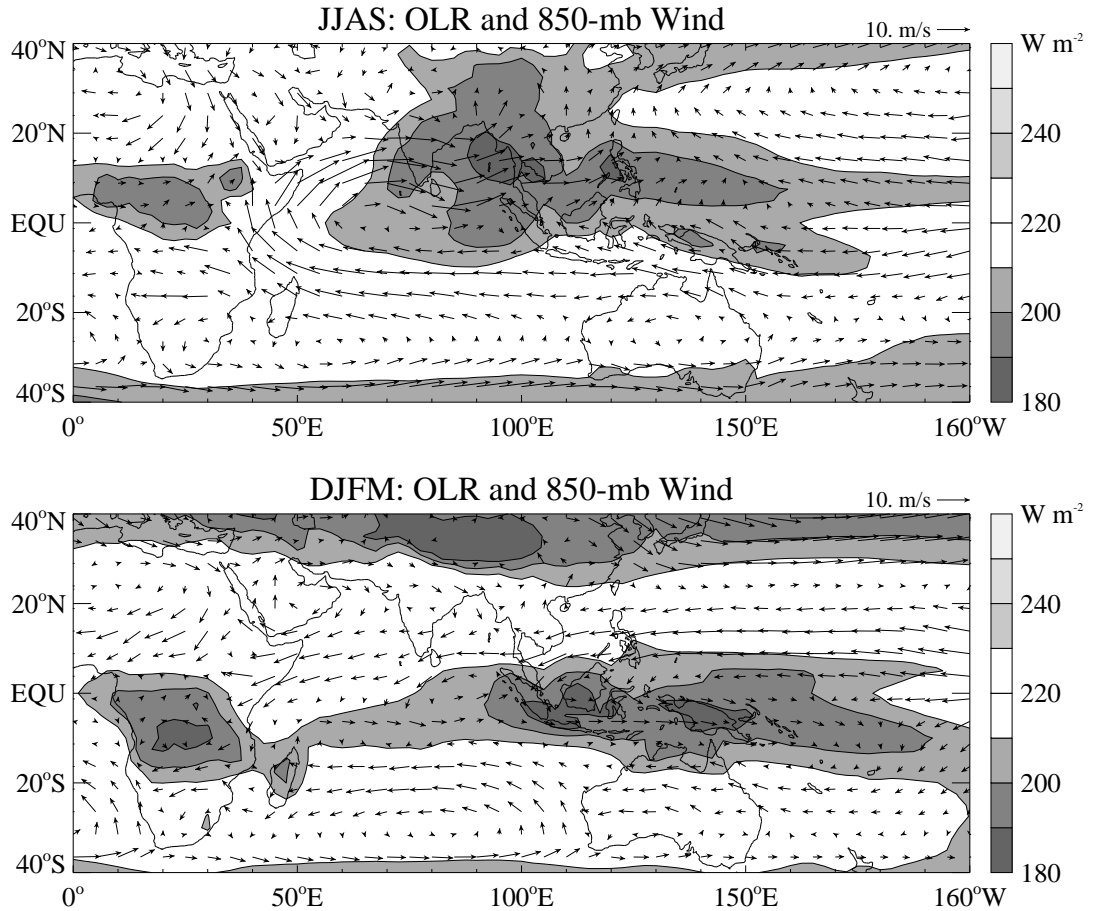


Figure 1.3. Climatology of OLR and 850-mb wind for 23 boreal summers (JJAS), 1975–1997 (excluding 1978 for OLR) and 23 boreal winters (DJFM), 1974–1997 (excluding 1977 and 1978 for OLR). Data from NOAA Outgoing Longwave Radiation dataset (Section 2.1.1) and NCEP/NCAR reanalysis (Section 2.1.2).

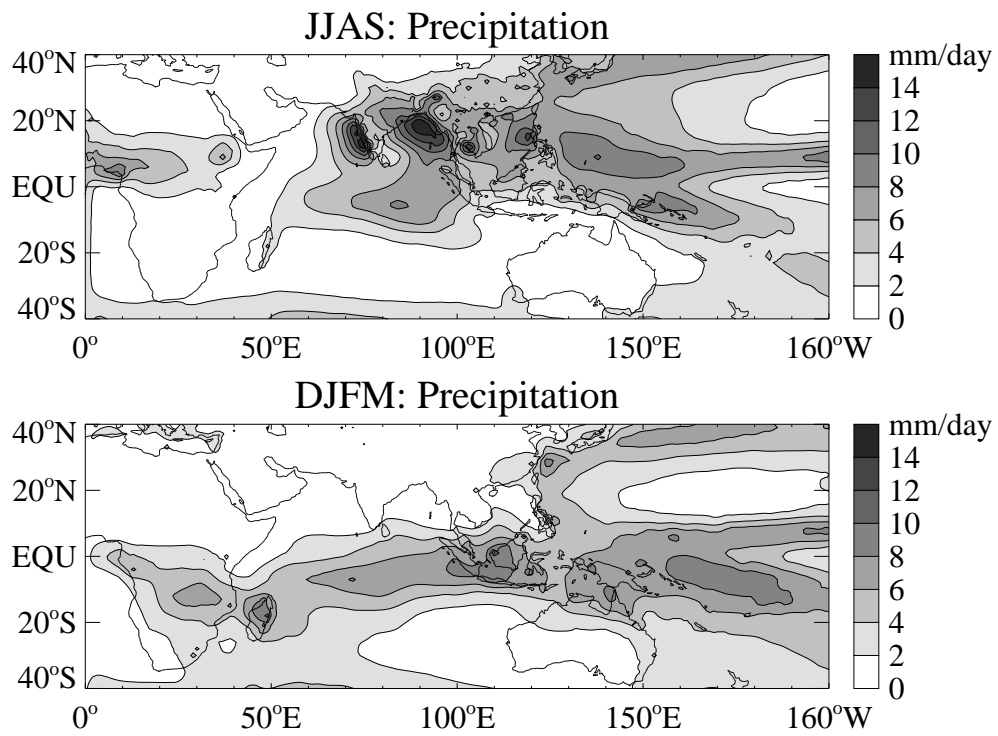


Figure 1.4. Climatology of precipitation estimates for 1979–1995 JJAS and DJFM. Precipitation estimates from station data over land and MSU satellite data over oceans (Section 2.1.4).

Fasullo and Webster 1999a). The relatively steady flux of moist, unstable air advected over the South Asian landmass supports deep convection and precipitation across the South Asian monsoon region. Mean summertime OLR less than  $220 \text{ W m}^{-2}$  (OLR values less than  $220 \text{ W m}^{-2}$  are generally considered to indicate rainfall, e.g. Arkin and Ardanuy (1989)) is located north of the equator over a large portion of the Asian monsoon region. The climatological summer rainfall (Fig. 1.4) is characterized by average daily precipitation rates exceeding  $5 \text{ mm day}^{-1}$  throughout the south and southeast Asian regions as well as through much of the northern Indian Ocean including the eastern Arabian Sea and especially the Bay of Bengal, where the highest mean precipitation rates in the entire monsoon are found. The areas of maximum precipitation tend to be located upstream of low, coastal mountains that induce low-level lifting of conditionally unstable air (Grossman and Durran 1984; Grossman and Garcia 1990). An intriguing maximum in precipitation is also found in the winter hemisphere just south of the equator at  $80^\circ\text{--}90^\circ\text{E}$ .

The mean convection and precipitation, during northern winter, shifts from southern Asia to along and south of the equator over the maritime continent and northern Australia and extending into the South Pacific Convergence Zone (SPCZ). The 850-mb circulation is now marked by north-easterly winds over the Indian subcontinent and cross-equatorial flow from north to south over the maritime continent which provides moisture for the Australian monsoon rainfall.

The boreal summer South Asian monsoon tends to be stronger than the boreal winter Australian monsoon both in terms of total precipitation and the strength of the monsoonal circulation. The differences are due in large part to the presence or absence of an elevated heat source. The South Asian monsoon is strongly influenced by the elevated Tibetan plateau heat source. The onset of the boreal

summer monsoon is coincident with the reversal of the meridional temperature gradient in the upper troposphere south of the Tibetan plateau (Flohn 1957; Li and Yanai 1996). The temperature gradients in the southern hemisphere never reverse due to the absence of an elevated heat source in Australia. However, there are still strong cross-equatorial pressure gradients that drive the boreal winter monsoon. The gradients, not as large as those occurring in the boreal summer, are the result of the intense radiational cooling over north Asia during winter (Webster *et al.* 1998).

The climatological 200-mb winds are shown in Fig. 1.5 for both the summer and winter seasons. The predominant feature is the persistent upper level westerly jets poleward of  $20^\circ$  in both hemispheres. Over South Asia and Africa, there is an upper level easterly jet during summer that is replaced by an upper level westerly jet during winter. Overall, the upper level flow in both seasons is largely opposite in direction to the low level flow yielding an easterly vertical wind shear during summer and a westerly vertical wind shear during winter. Cross-equatorial return flow is also evident during summer, a significant portion of which is divergent (not shown), and thus contributes to the local Hadley cell (Krishnamurti 1971).

The climatological SST distributions are shown in Fig. 1.6. Mean SSTs in excess of  $28^\circ\text{C}$  are confined to equatorial latitudes. In the Indian Ocean basin and the western Pacific Ocean, a clear latitudinal shift of warm SSTs into the summer hemisphere is evident. The entire Bay of Bengal and the eastern Arabian Sea possess warm SSTs during summer, extending from  $5^\circ\text{S}$  to the Bangladesh coast at  $20^\circ\text{N}$ . In winter, the area of warm SST is more evenly distributed about the equator, extending from  $10^\circ\text{N}$  to  $15^\circ\text{S}$ . Also of note is the expansion of warm SSTs eastward in the central equatorial Pacific Ocean and westward in the Indian Ocean during northern

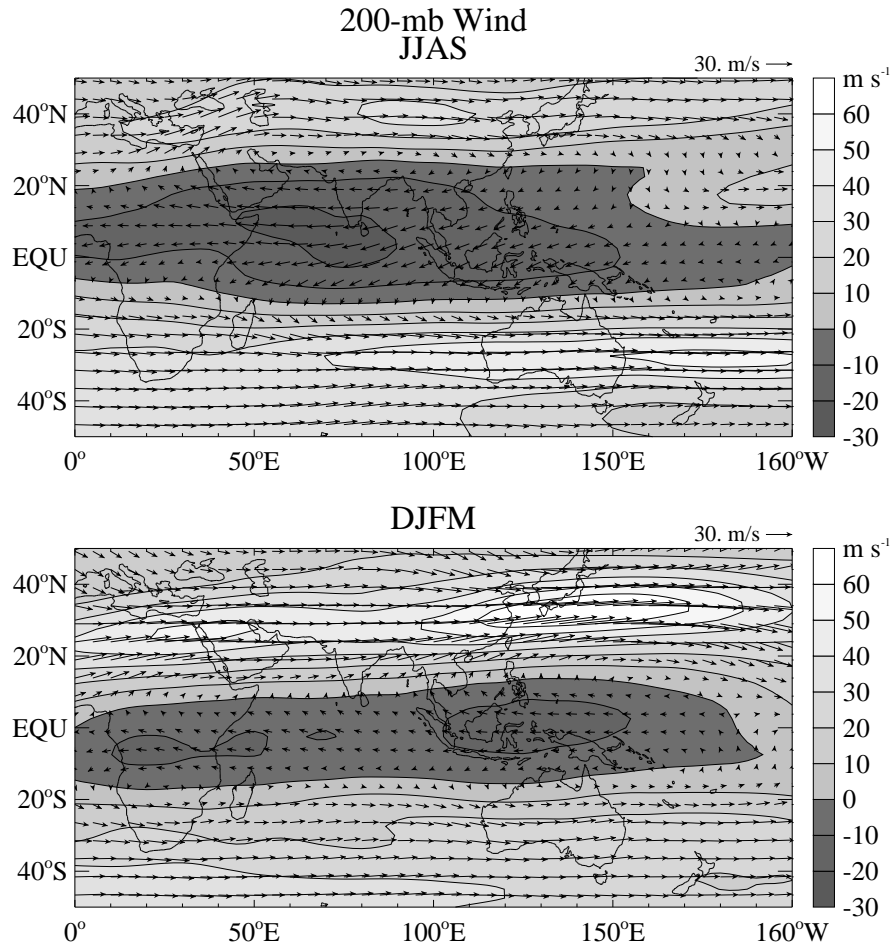


Figure 1.5. Climatology of 200-mb wind (vectors) and zonal 200-mb wind (contours) for 23 boreal summers (JJAS), 1975–1997 and 23 boreal winters (DJFM), 1974–1996. Winds from NCEP/NCAR reanalysis (Section 2.1.2).

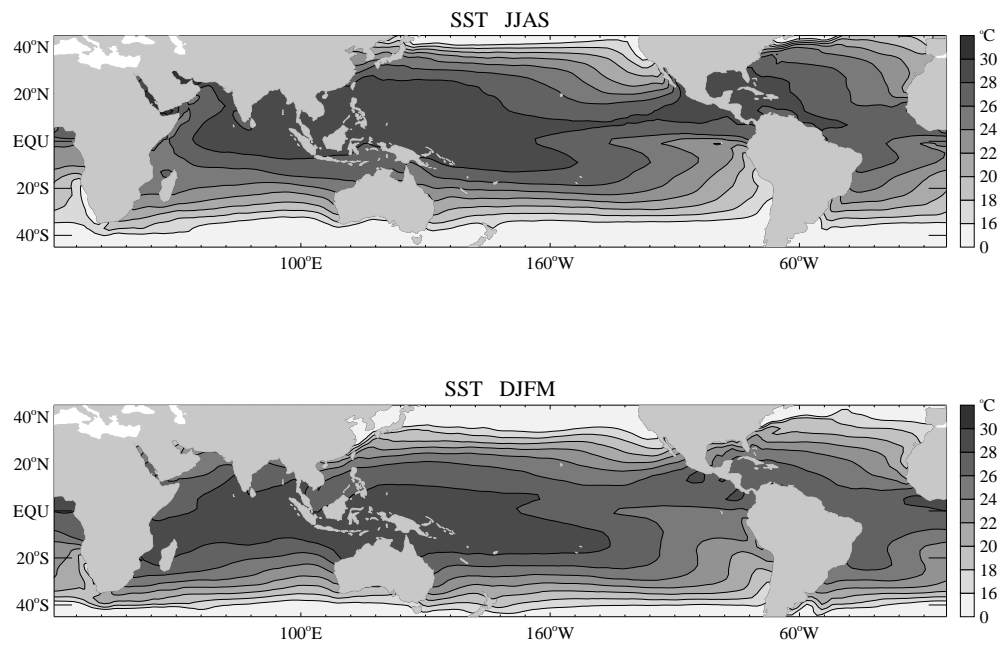


Figure 1.6. Climatology of SST for 16 summers (JJAS) and winters (DJFM), 1982–1997. SST from Reynolds sea surface temperature (Section 2.1.3).

winter. While the climatological SST distributions are presented here, there are also significant intraseasonal changes in SST that are important and which will be discussed in Section 3.2.2.

## 1.2 Variability of the South Asian Monsoon

**1.2.1 The Intraseasonal Oscillation** The southwest or South Asian monsoon is marked by episodes of prolonged abundant precipitation (active periods) separated by periods of prolonged reduced rainfall (break periods). The transitions from active to break periods and vice versa evolve slowly such that there are typically 3 to 4 active periods over the course of a single monsoon season, May to September (Webster *et al.* 1998). Prolonged dry spells at critical life stages are found to adversely affect crop development and growth, and hence yields (see e.g., Lal *et al.* 1999). Consequently, understanding the transitions as well as the timing of rainy and dry spells has sociological importance and is particularly relevant for farmers and water managers since advance information of forthcoming active and break spells could be used to implement agricultural and water management strategies.

The low-frequency active/break cycles occur on timescales of about 30–40 days (Raghavan *et al.* 1975; Yasunari 1979; Yasunari 1980; Yasunari 1981; Krishnamurti and Subrahmanyam 1982; Lau and Chan 1986; Gadgil and Asha 1992) with transitions between the two states taking about 15–20 days. Spectral peaks in monsoonal parameters have been found in the 30–40-day period band in a number of studies (e.g., Yasunari (1979), cloudiness; Cadet (1986), precipitable water; Knutson *et al.* (1986), OLR and  $u_{250}$ ; Hartmann and Michelsen (1989), precipitation). It will turn out not to be a coincidence that the period of oscillation is approximately

the same as that of the Madden-Julian Oscillation (MJO, Madden and Julian 1971; Madden and Julian 1972), also termed the Intraseasonal Oscillation (ISO).

Climatologically, the ISO is strongest during the boreal winter and spring seasons when it appears as a strictly eastwardly propagating large-scale system of convection along the equator, extending from the Indian Ocean east to the dateline (Hendon and Salby 1994). During the southwest Asian monsoon season, the ISO is typically weaker and of more complex character (Madden 1986). A fundamental and unique characteristic of the summer ISO is a northward propagation of convection, beginning in the central equatorial Indian Ocean and ending at the foot of the Himalayan mountains in northern India. The northward propagation of convection has been observed and described by many authors (e.g., Murakami 1976; Yasunari 1979; Yasunari 1980; Yasunari 1981; Sikka and Gadgil 1980; Krishnamurti and Subrahmanyam 1982; Singh and Kripalani 1985; Lau and Chan 1986; Wang and Rui 1990). The similarity between the timescale of the ISO and the cycling time from active to break to active period over India led Yasunari (1979), and subsequently Julian and Madden (1981) and Lau and Chan (1986), to suggest that the northward propagation of convection is associated with the eastward propagating clouds along the equator (for review see Madden and Julian 1994). Recently, Webster *et al.* (1998) observed that the northward propagation of precipitation from the equator is accompanied by a concomitant southward propagation of convection which lasts for a shorter duration and extends only to 15°S, which may explain why there is a climatological precipitation summer maximum south of the equator in the eastern Indian Ocean.



Many of these features can readily be seen in observations. Figure 1.7a is a time-latitude section of OLR anomalies along Indian peninsular longitudes,  $75^{\circ}$ – $85^{\circ}$ E, during June and July, 1996. Both northward and southward propagation of convection is evident in the raw data. Figure 1.7b is a time-longitude section along a latitudinal swath between the equator and  $5^{\circ}$ N. Two eastward propagating convective events occur during the 2-month period. During both events, the northward propagation of convection begins subsequent to the passing of a large-scale equatorial convective system. Figure 1.7c, a time-longitude section along  $10^{\circ}$ – $15^{\circ}$ N, suggests that this interpretation of the ISO evolution may be incorrect or incomplete because a west to east propagation of convection, that lags the eastward propagation of convection along the equator by about 5-10 days, is also apparent at these latitudes. One of the goals of this study is to interpret the off-equatorial eastward propagation in the context of known ISO dynamics.

**1.2.2 Other Intraseasonal Variability** The second intraseasonal mode that is prevalent during the Asian summer monsoon is composed of high-frequency, 5–10-day, wavelike phenomena, including westward propagating synoptic-scale vorticity waves (Lau and Lau 1990) as well as monsoon depressions and lows (for review see Mak 1987). These storms typically form in the Bay of Bengal or in the western Pacific Ocean and propagate westward and north-westward into the Ganges River valley (Krishnamurti *et al.* 1977; Saha *et al.* 1981). Large precipitation amounts accompany these disturbances and can lead to flooding, especially in the lowlands of northeast India and Bangladesh.

**1.2.3 Interannual Variability** The interannual variability of the South Asian monsoon has been the subject of extensive research (for review see

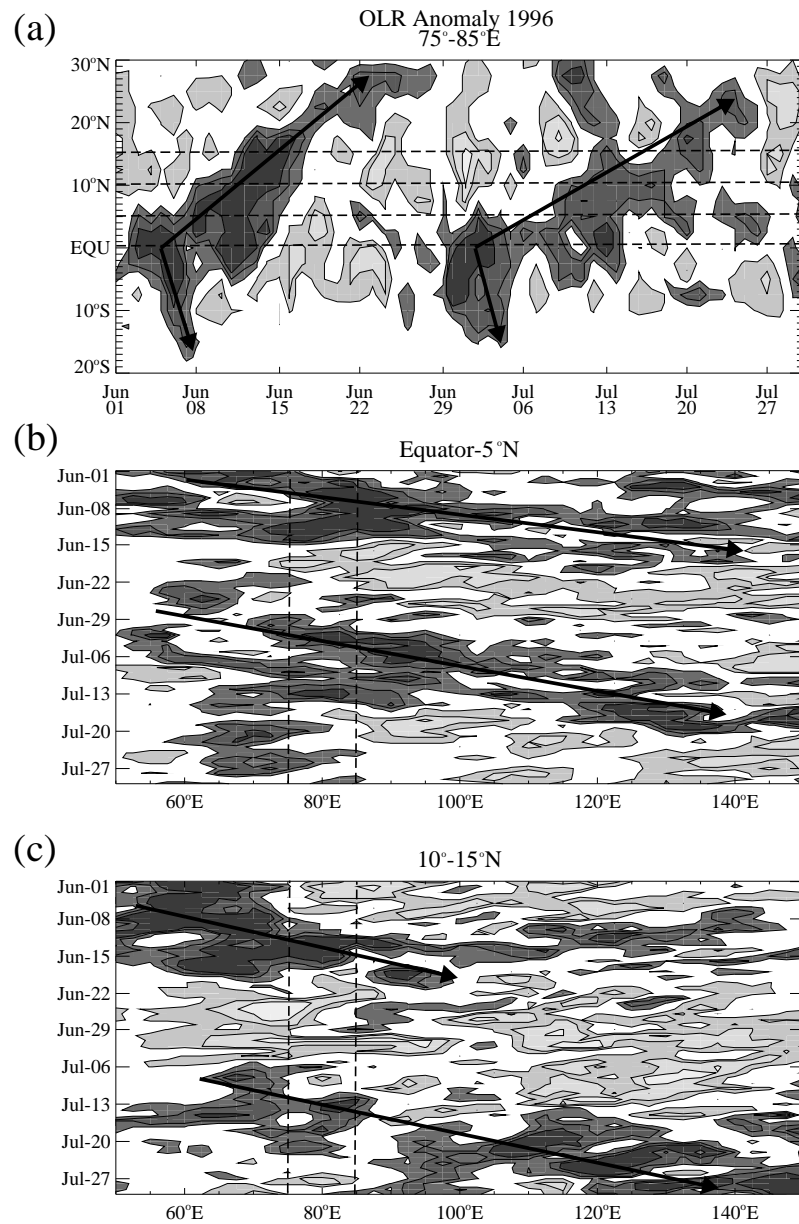


Figure 1.7. Time-space diagrams of raw OLR anomalies for June–July, 1996. Anomalies are calculated by removing the mean and the first three harmonics of the annual cycle (365.25, 182.625, and 121.75 days). Contour intervals are every  $20 \text{ W m}^{-2}$  with dark shades indicating negative OLR anomalies and light shades indicating positive OLR anomalies. OLR anomalies are averaged along (a) 75°–85°E, (b) Equator – 5°N, (c) 10°–15°N.

Webster *et al.* 1998). A number of studies have investigated the complex relationship between eastern Pacific SSTs and Indian monsoon strength (e.g., Webster and Yang 1992; Ju and Slingo 1995; Wainer and Webster 1996). Although the separation of cause and effect is difficult, a warm ENSO event tends to suppress monsoon convection (Webster 1995) while, conversely, a strong monsoon tends to inhibit warm ENSO events (Yasunari 1990). Further complicating the monsoon-ENSO relationship is that it appears to possess interdecadal variability (Elliot and Angell 1988; Torrence and Webster 1999).

Webster *et al.* (1998) point out that nearly all El Niño years are drought years in India but not all drought years correspond to El Niño years. Therefore, although the ENSO-monsoon relationship appears strong it does not explain all the interannual variance of monsoon strength. Consequently, other sources of interannual monsoon variability have been sought including links between monsoon strength and other SST anomalies. A number of studies show strong positive lead correlations between Indian Ocean SST and Indian rainfall (e.g., average March-May Arabian Sea SST, Rao and Goswami (1988); preceding fall and winter Indian Ocean SST, Harzallah and Sadourny (1997) and Clark *et al.* (1999)).

Apart from the ENSO timescale, the monsoon exhibits distinct biennial fluctuations (Mooley and Parthasarathy 1984). The biennial component may be related to the tropospheric biennial oscillation (TBO) that is found in many atmospheric variables including precipitation, surface pressure, tropospheric winds, and SST (Meehl 1987; Meehl 1997) or to biennial variations in Eurasian snow cover (Vernekar *et al.* 1995; Yang 1996).

### **1.3 Summary**

The mean monsoon and the annual cycle, with emphasis on the differences between the boreal summer and winter, in rainfall distribution, OLR, circulation, and SST have been described (Figs. 1.3–1.6). Evidence of the wide-ranging variability of the South Asian monsoon from synoptic to interannual variability was presented (Figs. 1.1–1.7). The current understanding of the summertime ISO, synoptic-scale variability, and interannual variability of the South Asian monsoon was reviewed.

The next chapter examines the large-scale structure and evolution of the summer ISO, the dominant mode of intraseasonal variability in the South Asian monsoon.